scientific reports

Check for updates

OPEN

Optimizing wind turbine blade pitch control via input output differential model free adaptive control

Ziang Zhou[1], Shuangxin Wang[1]✉, Jiading Jiang[2], Hongrui Li[1], Juchao Zhao[1] & Dingli Yu[3]

In the context of wind energy systems, maintaining optimal power output in wind turbines when wind speeds exceed rated values necessitates precise regulation of blade pitch through the pitch control system. However, challenges in accurately modeling nonlinear control systems and enhancing control responsiveness arise due to factors such as actuator constraints, unmodeled dynamics, and random wind speed fluctuations. This paper proposes an improved model free control, termed Input Output Model Free Adaptive Control (IO-MFAC). It enhances the system's adaptability to stochastic wind and improves tracking capabilities by adaptively adjusting the input difference based on the output difference through the new cost function. Moreover, to demonstrate the stability of IO-MFAC, its monotonic convergence is theoretically confirmed. Simulations conducted on the FAST simulator and hardware-in-the-loop experiments demonstrate that IO-MFAC outperforms basic MFAC under constant wind and turbulent conditions, exhibiting superior dynamic tracking performance, control effectiveness, and practical utility.

Wind energy is a vital renewable resource due to its abundant availability and potential. However, the variable nature of wind, combined with the complexities of wind turbine systems, presents significant challenges in effectively harnessing this energy. To manage these challenges, control strategies are implemented to adjust the blade pitch angle, particularly when wind speeds exceed the turbine's rated capacity. This adjustment is crucial for stabilizing power output and preventing damage to essential components during high wind conditions[1]. Consequently, effective blade control is central to maintaining the reliability of wind power systems.

Various control strategies have been employed in variable pitch control. These include the Proportional-Integral (PI) method[2], which combines proportional and integral terms for enhanced performance; the Linear Quadratic Gaussian (LQG) approach[3], which utilizes quadratic optimization and accounts for Gaussian noise; and Model Predictive Control (MPC)[4], which optimizes control inputs by predicting system behavior over a finite time horizon. Other methods, such as finite-time continuous nonsingular terminal synergetic control[5], enhance robustness under actuator faults, while L1 adaptive schemes[6] improve pitch angle control stability in Permanent Magnet Synchronous Generator (PMSG) wind turbine systems; and the Robust Control method[7], designed to handle uncertainties and disturbances for enhanced system stability. However, these algorithms heavily rely on accurate models of the control systems. For instance, Robust Control methods necessitate prior mathematical modeling of wind turbines and an understanding of uncertain dynamics[8]. Additionally, LQG and PI approaches are limited by their reliance on specific operating point models, making them less responsive to changes in system data[9]. As systems grow increasingly complex and nonlinear, creating precise controller models becomes more difficult, and model-based methods often face limitations due to unmodeled dynamics.

To tackle these modeling challenges, artificial intelligence (AI) control methods have also emerged. Notably, a novel reinforcement learning (RL) controller that integrates deep neural networks (DNNs) with MPC has shown significant improvements in the robustness and performance of wind turbine control systems, particularly under uncertain conditions and actuator failures[10]. Additionally, a fractional-order fuzzy control (FOFC) method has proven effective in enhancing the robustness of doubly-fed induction generator (DFIG)-based wind energy systems, outperforming traditional Direct Power Control (DPC) strategies in mitigating power ripple and

[1]School of Mechanical, Electronic and Control Engineering, Beijing Jiaotong University, 3 Shangyuan Village, Haidian, Beijing 100044, China. [2]School of Energy Engineering, Xinjiang Institute of Engineering, Ürümqi 830023, China. [3]Control Systems Center, School of Engineering, Liverpool John Moores University, Liverpool L3 3AF, UK. ✉email: shxwang1@bjtu.edu.cn

harmonic distortion[11]. However, these AI-based approaches often require extensive training data and time, and may lack interpretability, creating challenges in their practical application.

In light of these issues, model-free adaptive control (MFAC) methods, which depend on real-time system data rather than mathematical models, have gained attention in recent research[12]. MFAC has been successfully applied in various fields, including distributed collaborative tracking in multi-agent systems (MAS)[13], crane load sway management[14], reactive power compensation[15], and inverter synchronization[16]. Nonetheless, there remains limited research on its application to stochastic wind energy[17], highlighting the need for further investigation in this area.

Recent advancements in MFAC have led to notable improvements. For instance, Huang et al.[18] developed a Differential Evolution and Sliding Mode Control strategy for Full-Form Dynamic Linearization Model-Independent Adaptive Control (DESO-based FFDL MFAC), which effectively addresses trajectory tracking for wheeled mobile robots. Li et al.[19] integrated fuzzy optimization with MFAC for underwater vehicle heading control, demonstrating its effectiveness through simulations and experiments. Similarly, Yu et al.[20] enhanced the dynamic linearization of MFAC using neural networks, confirming its application for controlling Piezoelectric Micro-Positioning (PMP) platforms. Liu et al.[21] combined MFAC with reinforcement learning to improve robustness and tracking accuracy. Xu et al.[22] employed a particle swarm optimization strategy with recurrent neural networks to enhance stability in Czochralski-grown silicon crystal production. While these developments improve the performance of basic MFAC, they also introduce high computational complexity and constraints in specific applications, indicating a need for further research to enhance their generality and practicality.

Considering the inherent variability of stochastic wind energy in variable-pitch systems, this paper proposes a novel enhanced data-driven model-free control method. By monitoring real-time input and output error rates and adjusting the blade pitch angle accordingly, we improve the system's adaptability to changes in wind energy. This approach improves the controller's ability to track generator speed variations without requiring precise system modeling, reducing computational complexity and enhancing general applicability.

The mathematical formulation derivation of IO-MFAC

Figure 1 illustrates the overall structure of IO-MFAC, where the symbol Z^{-1} denotes the backward temporal shift. The module labeled as D&M incorporates the principles of difference and memory.

The mathematical form of basic-MFAC

The classical discrete-time nonlinear system with a single-input single-output (SISO) configuration can be expressed as follows:

$$y(k+1) = f\left(y(k), \cdots, y\left(k-n_y\right), u(k), \cdots, u\left(k-n_u\right)\right). \tag{1}$$

In this representation, $u(k) \in \mathbb{R}$ denotes the system input at time k, and $y(k) \in \mathbb{R}$ represents the corresponding output. The parameters n_y and n_u are positive integers with uncertainty. Additionally, $f(\cdot) : \mathrm{R}^{n_u+n_y+2} \rightarrow \mathrm{R}$ characterizes an uncertain nonlinear function governing the system dynamics.

For convenience in subsequent discussions, we make two reasonable assumptions about the SISO system:

1. With the exception of a finite set of time points, the continuity of the partial derivative of $f(\cdot)$ concerning the (n_y+2)th variable is maintained. this assumption is generally practical, as most physical systems, including wind turbines, tend to have smooth response characteristics.
2. With the exception of a finite set of time points, the SISO system adheres to the generalized Lipschitz condition. This implies that, for any $k_1 \neq k_2, k_1, k_2 \geq 0$, and $u(k_1) \neq u(k_2)$, the following condition is met:

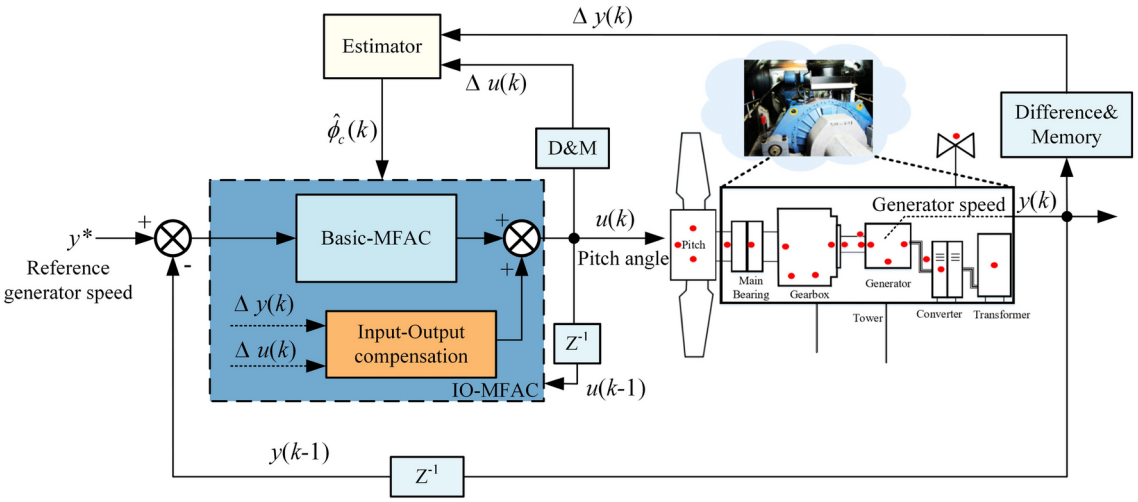

Fig. 1. Overall structure of the IO-MFAC.

$$|y(k_1+1)-y(k_2+1)| \le b\,|u(k_1)-u(k_2)|, \tag{2}$$

with $b > 0$ as a constant.The Lipschitz condition suggests that the system's output is predictable and stable relative to its input. In practice, this condition can usually be met by controlling the input signal and using appropriate filtering, as demonstrated in many real-world systems.

Given the aforementioned assumptions, it is possible to convert the SISO system into a concise form using dynamic linearization, often referred to as the Compact Form Dynamic Linearization (CFDL) model[23]:

$$y(k+1) = \phi_c(k)\Delta u(k) + y(k), \tag{3}$$

where $\Delta u(k) = u(k) - u(k-1)$ and $\phi_c(k) \in \mathrm{R}$ is the bounded pseudo partial derivative (PPD).

When dealing with discrete-time systems, control algorithms often adjust system behavior by minimizing the cost function associated with prediction errors. However, excessive focus on one-step prediction errors can lead to unnecessary control inputs, potentially causing harm to the overall system. Additionally, introducing a cost function with weighted one-step prediction errors may introduce errors during steady-state. Therefore, to address these issues, the following cost function is introduced:

$$J(u(k)) = (y^*(k+1) - y(k+1))^2 + \lambda(u(k) - u(k-1))^2, \tag{4}$$

where $y^*(k+1)$ is the reference of output; $\lambda > 0$ is a weighting factor.

By deriving Eq. (4) partially concerning $u(k)$ and equating it to zero, we derive the optimal control input as follows:

$$u(k) = u(k-1) + \frac{\rho\phi_c(k)}{\lambda + |\phi_c(k)|^2}\left(y^*(k+1) - y(k)\right). \tag{5}$$

Here, we introduce the step factor $\rho \in (0, 1]$ to provide a more generalized form for this algorithm.

Given that PPD is a parameter that varies with time and obtaining its actual value poses challenges, an estimation approach has been employed to approximate PPD. The consideration involves the utilization of the following criterion function for PPD estimation:

$$J(\phi_c(k)) = (y(k) - y(k-1) - \phi_c(k)\Delta u(k-1))^2 + \mu(\phi_c(k) - \hat{\phi}_c(k))^2, \tag{6}$$

where $\mu > 0$.

We take the derivative of (6) with respect to $\phi_c(k)$, and note that the extreme value point of $J(\phi_c(k))$ is the estimated value $\hat{\phi}_c(k)$,

$$\hat{\phi}_c(k) : \phi_c(k) = \hat{\phi}_c(k-1) + \tfrac{\eta\Delta u(k-1)}{\mu+\Delta u(k-1)^2}(\Delta y(k) - \hat{\phi}_c(k-1)\Delta u(k-1)), \tag{7}$$

where $\eta \in (0, 1]$ denotes step factor and $\mu > 0$. If either $|\hat{\phi}_c(k)| \le \varepsilon$, $\Delta u(k-1) \le \varepsilon$, or $\mathrm{sign}(\hat{\phi}_c(k)) \ne \mathrm{sign}(\hat{\phi}_c(1))$ is true, then $\hat{\phi}_c(k)$ is set to $\hat{\phi}_c(1)$. Here, $\hat{\phi}_c(1)$ represents the initial value, and ε is a sufficiently small positive constant.

Using historical data, we obtain $\hat{\phi}_c(k)$ through Formula (7), and by guiding Formula (5) with it, we derive the final control input, achieving model free control relying solely on data. Organizing the above equation, the final control input for basic-MFAC is

$$u(k) = u(k-1) + \frac{\rho\hat{\phi}_c(k)}{\lambda + \left|\hat{\phi}_c(k)\right|^2}\left(y^*(k+1) - y(k)\right). \tag{8}$$

The mathematical formulation of IO-MFAC

The rotational speed of wind turbines fluctuates significantly due to the unpredictable nature of wind. Concurrently, basic-MFAC faces conflicting demands of responsiveness and tracking arising from constraints in actuators, the inertia of the system, and delays in time[24]. This conflict intensifies because the squared difference term of the control input in Function (4) does not adaptively account for the variations in output between adjacent moments, leading to basic-MFAC's inability to accurately modulate blade pitch angles in response to fluctuations in generator speed caused by wind velocity changes. To address this limitation and enhance the modeling and tracking performance of basic-MFAC, we propose an IO-MFAC strategy that considers the mutual influence of input and output variations. A new cost function for control input is formulated as follows:

$$\begin{aligned} J(u(k)) = {} & (y^*(k+1) - y(k+1))^2 + \lambda(u(k) - u(k-1))^2 \\ & + \alpha(y(k+1) - y(k) - \beta(u(k) - u(k-1)))^2. \end{aligned} \tag{9}$$

Equation (9) indicates that to minimize the last term in the cost function, the system must rapidly adjust the input differences to counterbalance substantial variations in output between consecutive time steps. This constraint

allows the controller to dynamically adapt the inputs based on the output variations, thereby enhancing the system's ability to achieve precise state tracking.

In combination with (7), we derive the derivative of (9) for $u(k)$ to obtain the optimal $J(u(k))$. The IO-MFAC is obtained

$$\begin{aligned} u(k) = u(k-1) + \frac{\rho\hat{\phi}_c(k)}{\lambda + (\hat{\phi}_c(k))^2 + \alpha(\hat{\phi}_c(k) - \beta)^2}(y^*(k+1) - y(k)) \\ - \frac{\alpha\left\{[y(k) - y(k-1)] - \hat{\phi}_c(k-1)[u(k-1) - u(k-2)]\right\}[\hat{\phi}_c(k) - \beta]}{\lambda + (\hat{\phi}_c(k))^2 + \alpha[\hat{\phi}_c(k) - \beta]^2}. \end{aligned} \tag{10}$$

While this formulation incorporates the necessary adjustments for effective control, a more detailed explanation of each step, along with a simplified representation where possible, could further enhance understanding. For instance, highlighting the roles of parameters such as ρ, γ, and α in tuning the control response could clarify their impact on system behavior.

Stability proof

Formulated for the meticulous scrutiny of stability, the assumptions are postulated for the System 1 as follows[25]:

1. Given a bounded expected output $y^*(k+1)$, existing a bounded control input $u^*(k)$, such that the system output equals to $y^*(k+1)$ with the impact of this input. Although wind speed is highly random, a reasonable control strategy can ensure that the system input and output remain within the expected range, thus satisfying the boundedness condition. This is crucial for ensuring the stable operation of the wind turbine and extending its lifespan.
2. For any non-zero $\Delta u(k)$, the positive and negative signs of PDD remain consistent, and it satisfies $|\phi_c(k)| > \varepsilon$, where ε denotes a small positive value. It ensures that the system has sufficient driving force during the control process, avoiding control failures due to excessively small input changes. This assumption can be achieved in practical control design by adjusting control gains and filter parameters, ensuring that the system's response has the expected stability and predictability.

Without loss of generality, we set $\phi_c(k) > \varepsilon$ in this paper.

Moreover, these assumptions help simplify mathematical analysis, making the stability proof more rigorous and feasible. However, we also recognize that in certain extreme conditions, there may be a few cases where these assumptions are not fully met.Therefore, future experiments and simulation studies will further verify the applicability of these assumptions in real-world applications and explore the system's performance when the assumptions are not fully satisfied.

Simulation and results

We construct the simulation model in this section. Subsequently, our experiments are primarily divided into four dimensions. Firstly, the preliminary viability of IO-MFAC under steady wind speed is validated. Secondly, the experiment is conducted on the impact of hyper-parameter values on control performance. Thirdly, a comparison with classical control algorithms is undertaken to validate the tracking performance of IO-MFAC. Lastly, the feasibility of the algorithm is verified through hardware-in-the-loop experiments.

Simulation modeling

This paper employs the Simulink joint fatigue, aerodynamics, structure, and turbulence (FAST)[26,27] to implement basic-MFAC, and IO-MFAC. Developed by the National Renewable Energy Laboratory, the FAST software excels in constructing a wind turbine simulation environment with high precision. This study employs the 5 MW benchmark wind turbine from FAST as the experimental simulation. This wind turbine, rated at 5 megawatts, is equipped with three blades, each boasting a 126-meter diameter. Comprising the wind rotor, gearbox, and generator, the wind turbine's pitch system is equipped with a standard pitch controller (baseline PI) and a torque controller[28]. Refer to Table 1 for additional parameters.

Parameters	Value
Rated power	5 MW
Rotor orientation, configuration	Upwind, 3 Blades
Rotor, hub diameter	126 m, 3 m
Cut-in, rated, cut-out wind speed	3 m/s, 11.4 m/s, 25 m/s
Cut-in, rated rotor speed	6.9 rpm, 12.1 rpm
Rotor mass	110,000 kg
Nacelle mass	240,000 kg
Tower mass	347,460 kg

Table 1. Main parameters of the 5 MW wind turbine.

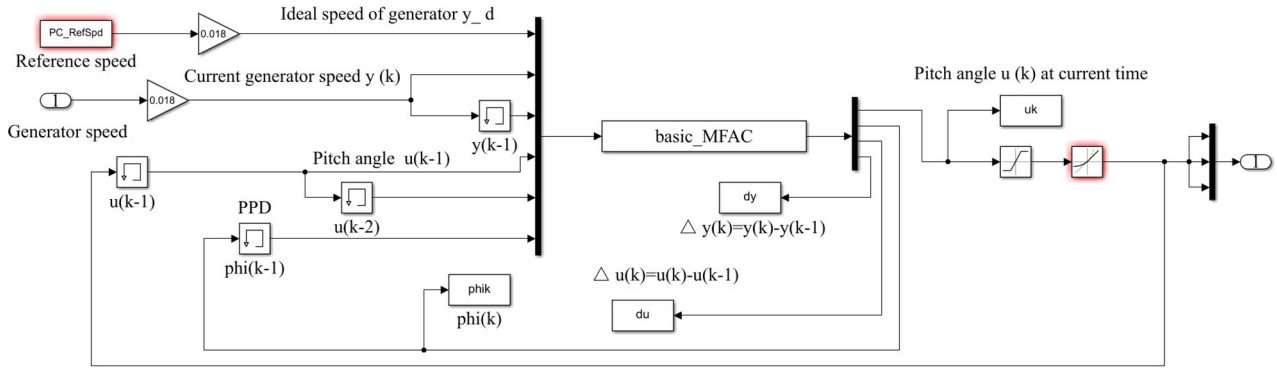

Fig. 2. Pitch controller based on IO-MFAC control of Simulink.

Parameter	Description	IO-MFAC	Basic-MFAC	PI
η	Cost function step factor	0.200	0.800	None
μ	PPD weight factor	0.001	1×10^{-5}	None
λ	Cost function weight factor	2.000	40.000	None
ρ	PPD step factor	0.015	0.001	None
α	Input Output step factor	8.000	None	None
β	Input step factor	1.000	None	None
$\phi_c(1)$	Initial PPD	10.000	10.000	None
$u(1)$	Initial input pitch angle	0.000	0.000	None
$y(1)$	Initial output generator speed	0.000	0.000	None
K_p	Scale factor	None	None	0.0081
K_i	Integral factor	None	None	0.110

Table 2. Parameters of the controllers.

The baseline PI controller, as a proportional-integral controller, has been thoroughly examined and adopted as the benchmark controller[28–30]. In order to ensure fairness and evaluate the controller's uniformity in the simulation environment, we choose the baseline PI as the benchmark for the controller. Furthermore, we exclusively modify the pitch controller, keeping all other parameters at their default values.

Figure 2 illustrates the Simulink model of the controller, while Table 2 outlines the parameters of the controller. These parameters have been carefully selected to achieve optimal performance.

Control performance under steady wind conditions

Utilizing the designed IO-MFAC variable-pitch controller, simulation is conducted in the Simulink/FAST platform. The total simulation duration is set at 100 s, employing a constant wind speed of 15 m/s. Given that the wind speed of 15 m/s exceeds the rated wind speed for the turbine, the ideal operational state of the turbine should involve maintaining a power output near the rated power of 5 MW. Additionally, the generator speed of the turbine is expected to remain in proximity to the rated speed of 123 rad/s. The wind turbine's power output, generator speed, generator torque, and pitch angle are depicted in Fig. 3.

From the simulation results, it is evident that the system enters a stable state after 20 s of simulation. The designed IO-MFAC controller effectively maintains the power output of around 5 MW, and the generator speed stabilizes near the reference value of 123 rad/s. It is observable that the designed IO-MFAC controller enables the wind turbine to stably track parameters such as power output and generator speed under steady-state wind conditions in the third operating condition.

The impact of selecting various α and β values on the performance of control

The IO-MFAC designs parameters α and β aimed at enhancing the performance in tracking generator speed while maintaining generality in the algorithm. Under conditions of turbulence, characterized by an average wind speed of 15 m/s (Fig. 4), simulations are conducted to assess the impact of varying α and β values on the presented algorithm. The parameters α and β are configured as 7, 6, 8, and 2, 1, 0.5, respectively. Figure 5 illustrates the variations in final power output and generator speed tracking performance.

Figure 5a, b reveals that the choice of α directly impacts the controller's tracking performance. Additionally, the sensitivity in error bias and power variations is inversely correlated with the value of α. As shown in Fig. 5c, d, it is evident that for $\beta \in (1, 2)$, decreasing the parameter value results in more stable power control and generator speed closer to the ideal speed.

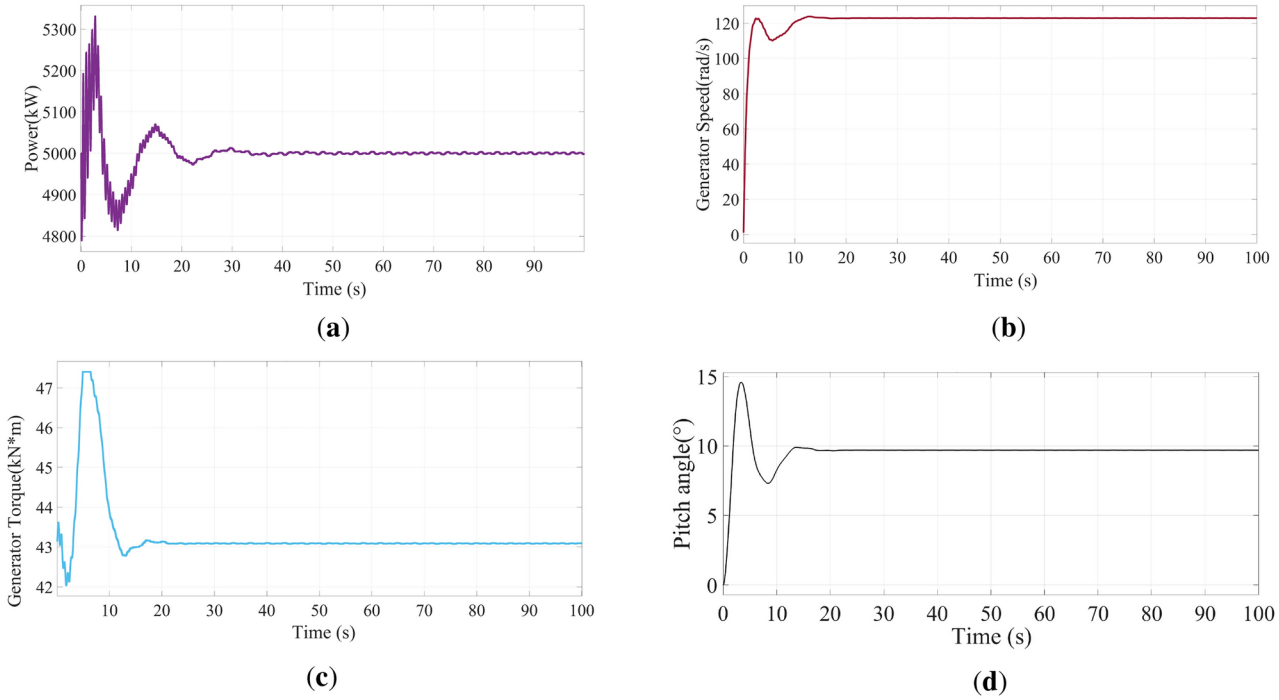

Fig. 3. Results of IO-MFAC under stable wind conditions: (**a**) power, (**b**) generator rotational speed, (**c**) torque, (**d**) angle.

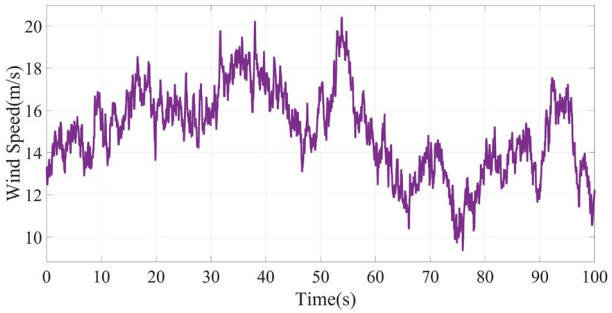

Fig. 4. Turbulent wind simulation.

Comparison with classical control algorithms

Comparison in the stable wind condition

First, simulations between different algorithms are performed at a constant wind speed of 15 m/s. At 15 m/s, the wind turbine operates in the third operating condition, i.e., the constant power control stage.

The operational parameters of the wind turbine under the three controllers are shown in Fig. 6. It can be seen from Fig. 6 that the basic-MFAC controller has a large overshoot and a long adjustment time, and it is almost impossible to play a role in the wind turbine pitch system. Compared with the PI controller, the IO-MFAC controller has faster response speed, reduced overshoot, and swift adjustment capabilities in power, rotational speed, and pitch angle control.

Results are compared in Table 3. It can be seen that at the constant wind speed of 15 m/s, the IO-MFAC control algorithm has smaller power error, generator speed error, power standard error(PSE), and generator speed standard error(GSE) than the PI control and the basic-MFAC control. The overshoot and adjustment time of the IO-MFAC are reduced by 35.4% and 49 s on average compared with the other two controllers, so it has a better performance.

Comparison in the turbulent wind condition

We conduct comparative experiments using the turbulent wind depicted in Fig. 4. In this environment, except for a slight decrease in wind speed around the 65th and 75th s, the wind speed remains above the rated speed for the remaining duration. Moreover, the wind possesses significant unpredictability and turbulence. We use

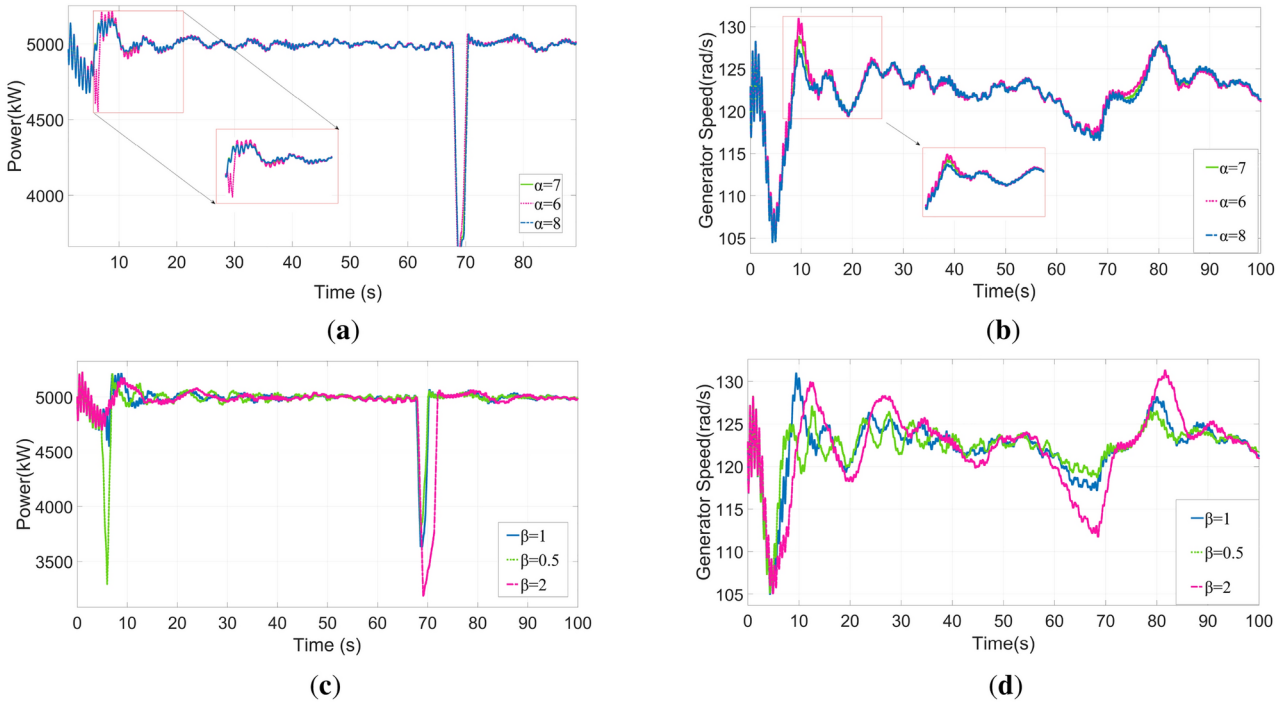

Fig. 5. The tracking performance of generator speed and power under different values of α and β. (**a**) Power; (**b**) generator rotational speed; (**c**) power; (**d**) generator rotational speed.

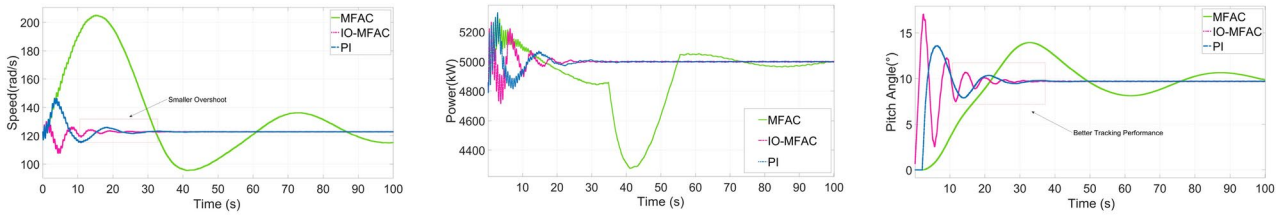

Fig. 6. Response of different controllers under the steady wind speed: (**a**) Generator rotational speed, (**b**) power, (**c**) angle.

Performance Index	PI	Basic-MFAC	IO-MFAC
Mean power (kW)	4999	4999	4900
Rated power (kW)	5000.00	5000.00	5000.00
Power error (kW)	1.00	100.00	1.00
Power standard deviation (kW)	42.44	245.55	39.01
Mean generator speed (rad/s)	123.46	135.36	122.56
Generator reference speed (rad/s)	122.9	122.9	122.9
Generator speed error (rad/s)	0.56	12.46	0.34
Standard deviation of generator speed (rad/s)	3.96	33.94	2.07
Adjustment time (s)	32	120	27
Overshoot (%)	20.83	66.67	8.33

Table 3. Comparison results of control performances for different methods under steady wind.

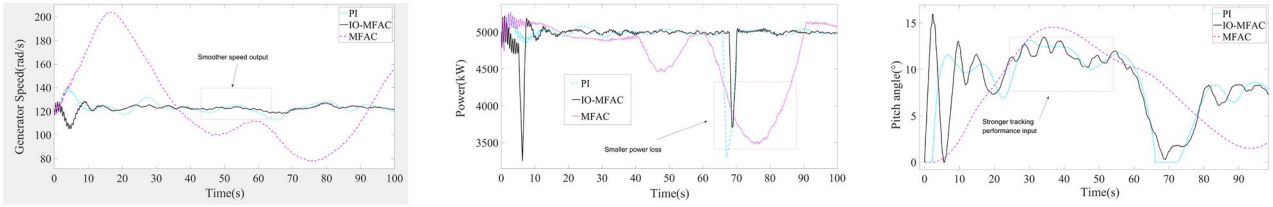

(**a**) (**b**) (**c**)

Fig. 7. Response of different controllers under the turbulent wind speed: (**a**) generator rotational speed, (**b**) power, (**c**) angle.

Performance index	PI	Basic-MFAC	IO-MFAC
Mean power (kW)	4950.00	4668.00	4957.00
Rated power (kW)	5000.00	5000.00	5000.00
Power error (kW)	50.00	332.00	43.00
Power standard deviation (kW)	249.95	600.72	209.22
Mean generator speed (rad/s)	123.27	126.19	122.38
Generator reference speed (rad/s)	122.90	122.90	122.90
Generator speed error (rad/s)	0.37	3.29	0.52
Standard deviation of generator speed (rad/s)	4.51	36.88	3.01

Table 4. Comparison results of control performances for different methods under turbulent wind.

PI and basic-MFAC as benchmarks for the comparative experiments. The experiments are conducted using simulations. And the results are presented in Fig. 7.

From Fig. 7a–c, it can be observed that IO-MFAC exhibits more exact speed output and quicker response. Furthermore, in turbulent conditions, due to its robust tracking performance, the method achieves better control performance through more blade movements.

Additionally, basic-MFAC struggles to adequately respond to rapid speed changes in turbulent wind speeds. This leads to substantial fluctuations in generator speed and power. In contrast, IO-MFAC rapidly reduces tracking errors induced by wind speed disturbances. Contrasted with the PI, IO-MFAC has lower generator speed fluctuations and maintains a more stable power level. At the 67th second in Fig. 7b, a sudden decrease in wind speed is observed. At this time, the IO-MFAC demonstrates a power reduction magnitude approximately two-thirds less than that of the baseline PI. This indicates that IO-MFAC exhibits stronger robustness under critical wind speed conditions.

We further quantify these control performances. Table 4 shows that PI has a slightly lower generator speed error than IO-MFAC control in terms of generator speed error. However, the IO-MFAC has a smaller power error, PSE, and GSE compared to PI and MFAC. In particular, when compared to the PI, the PSE and GSE of the IO-MFAC have decreased by 16.2% and 33.3%, respectively.

The Hil simulation of the IO-MFAC

To enhance the verification of the reliability and adaptability of IO-MFAC in real operational scenarios, a hardware-in-the-loop (HIL) simulation experiment is devised. Within the simulation, the tangible apparatus or environment is replaced by a simulated model interfaced with the authentic controller, thereby establishing a closed-loop test system. Moreover, intricate components resistant to mathematical modeling, such as converter systems, can be retained within the closed-loop system, facilitating controller testing within a laboratory setting[31].

As obtaining a real wind turbine experimental environment is challenging, only the wind turbine controller components are involved in the experiment. The IO-MFAC is transplanted onto the S7-1200 PLC for the HIL controller experiment, where the simulated wind turbine from FAST serves as the controlled object. Figure 8 shows the experimental setup.

In Fig. 9, It is evident that the IO-MFAC pitch controller demonstrates comparable trends in both experimental and simulation conditions. Hence, the performance of IO-MFAC in a semi-physical environment remains largely unaffected, showcasing a certain level of adaptability and reliability.

Discussion

From the simulation results, IO-MFAC demonstrates superior dynamic performance in both constant and turbulent wind conditions. In the presence of random wind speed disturbances, IO-MFAC exhibits smoother

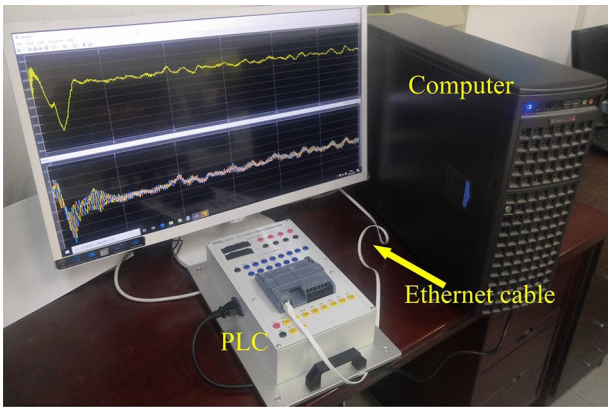

Fig. 8. HIL experimental system.

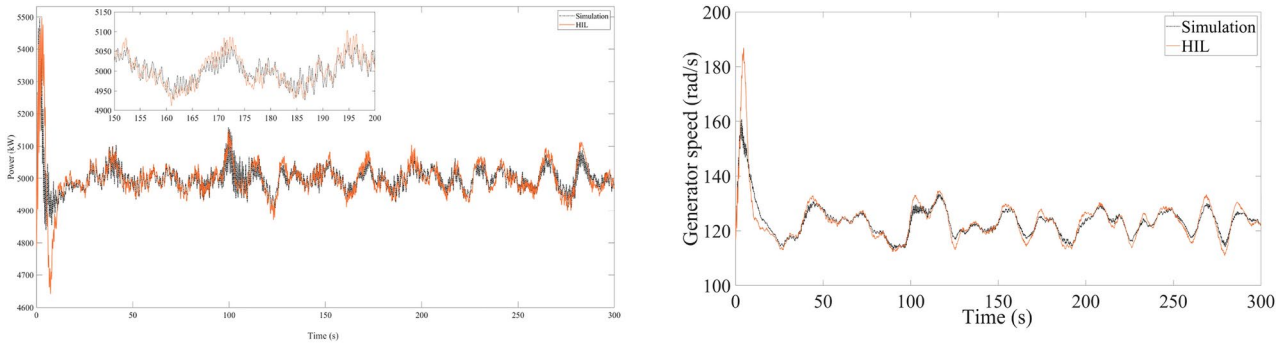

(**a**) (**b**)

Fig. 9. The HIL experiment versus simulation for collective pitch control utilizing IO-MFAC (**a**) power, (**b**) generator speed.

speed output and stronger tracking performance (see Fig. 6a, c). Contrastingly, achieving a balance between response speed and overshoot becomes challenging for basic-MFAC due to the impact of actuator constraints, system inertia, and time delays. Consequently, selecting and tuning parameters for basic-MFAC prove to be a challenging task. The results indicate that basic-MFAC can only achieve gradual stabilization in stable wind conditions but with a longer stabilization time, leading to insignificant fluctuations in power and generator speed. Additionally, in turbulent conditions, basic-MFAC fails to promptly suppress wind power fluctuations, especially during sudden changes in wind speed.

In turbulent wind conditions, although the baseline PI controller can accommodate changes in pitch angle, its tracking performance is inferior to IO-MFAC, leading to more power losses (see Fig. 7b). From the simulation results, we can infer that as wind speed continues to fluctuate, the PI controller, lacking strong nonlinear tracking capabilities, will further decrease the power absorption of the wind turbine. Hence, the baseline PI encounters difficulties in addressing the requirements of nonlinear control, as its control effectiveness is largely dependent on the stability of wind speed.

The IO-MFAC introduces new parameters α and β to adjust the system, aiming to address transient performance issues arising from the nonlinear system's varying time delays and inertia. In this manner, the burden on parameters ρ and λ can be alleviated, enhancing the flexibility in designing the controller and enabling a better balance between rapid response and high performance in the system.

Crucially, since IO-MFAC does not depend on specific modeling of a particular controlled system, the proposed approach is not just relevant for controlling wind turbine blades but is also well-suited for a category of control processes with similar characteristics like actuator constraints, significant inertia, and time delays. This aids the progress and implementation of the MFAC control theory. Furthermore, due to filter initialization and transient behavior during controlled system startup, there might be fluctuations in the initial simulation stages. However, compared to a wind turbine's operational time, these effects are minimal.

In the HIL experiment, the IO-MFAC exhibits results similar to those obtained under simulation conditions. This indicates that the controller exhibits good adaptability and reliability in a real hardware environment. Since hardware-in-the-loop experiments closely mimic actual working conditions, the consistency of results strengthens the credibility of IO-MFAC in practical applications. This consistency also provides a solid foundation for further extending and applying IO-MFAC to real wind power generation systems.

The findings of this study have to be seen in light of some limitations. Firstly, the examination of hyperparameter sensitivity is confined, the assessment may fail to capture the full extent of IO-MFAC's adaptability across diverse operational environments. The limited exploration of alternative tuning approaches could inadvertently obscure the algorithm's resilience in variable settings or neglect possible optimization avenues. Secondly, the study's investigation into the algorithm's impact on mechanical loads is incomplete. Rapid pitch angle modifications may escalate mechanical loads, a comprehensive assessment of these effects is lacking.

In future studies, we plan to conduct a more extensive sensitivity analysis of hyperparameters, explore alternative tuning methods, and perform a detailed evaluation of the mechanical load impacts associated with rapid pitch adjustments to further enhance the robustness and applicability of the IO-MFAC algorithm.

Conclusions

This paper introduces an enhanced model-free adaptive control (IO-MFAC) strategy for wind turbine pitch control, addressing model dependency and unmodeled dynamics typical in conventional controllers. By utilizing real-time input-output variation information, the IO-MFAC refines the cost function of standard MFAC, significantly improving tracking performance under stochastic wind conditions. The proposed algorithm achieves BIBO stability and monotonic convergence, with quantitative analysis showing a 16.2% reduction in the standard deviation of generator power and a 33.3% decrease in speed compared to basic-MFAC and baseline PI. Additionally, hardware-in-the-loop experiments confirm the practical applicability of IO-MFAC. Notably, this model-independent approach is relevant not only for wind turbine design but also for various control applications facing similar challenges. Future work will involve implementing IO-MFAC on a real wind turbine to further validate its performance.

Data availability

The datasets generated and analyzed during this study are available in the Science Data Bank (SciDB) repository. Reviewers can access the data anonymously via the read-only link:[https://www.scidb.cn/anonymous/MmlVcllm]. And the public access link is [https://www.scidb.cn/s/2iUrYf].

Code availability

The simulation code and analysis scripts used in this study are available in the Science Data Bank (SciDB) repository. During the peer review process, reviewers can access the code anonymously via the read-only link: [https://www.scidb.cn/anonymous/MmlVcllm]. Upon publication, the code will be publicly accessible at [https://www.scidb.cn/s/2iUrYf].

Received: 20 May 2024; Accepted: 30 January 2025
Published online: 21 February 2025

References

1. Tang, J., Dai, K., Luo, Y., Bezabeh, M. A. & Ding, Z. Integrated control strategy for the vibration mitigation of wind turbines based on pitch angle control and tmdi systems. *Eng. Struct.* **303**, 117529. https://doi.org/10.1016/j.engstruct.2024.117529 (2024).
2. Labed, N. et al. Pso based fractional order pi controller and anfis algorithm for wind turbine system control and diagnosis. *J. Electr. Eng. Technol.* **18**, 2457–2468. https://doi.org/10.1007/s42835-022-01330-w (2023).
3. de Lima Jr, J. C., Trentini, R. & Prioste, F. Comparative study of the pitch control of a wind turbine using linear quadratic gaussian and the unrestricted horizon predictive controller. *Int. Trans. Electr. Energy Syst.* **31**, e12721 (2021).
4. Ondes, E. B., Sultan, C., Hasankhani, A., VanZwieten, J. H. & Xiros, N. I. υ-gap metric based multi-model predictive control of an ocean current turbine system with blade pitch failures. *Ocean Eng.* **278**, 114201. https://doi.org/10.1016/j.oceaneng.2023.114201 (2023).
5. Palanimuthu, K. & Joo, Y. H. Reliability improvement of the large-scale wind turbines with actuator faults using a robust fault-tolerant synergetic pitch control. *Renew. Energy* **217**, 119164. https://doi.org/10.1016/j.renene.2023.119164 (2023).
6. Venkateswaran, R., Lee, S. R. & Joo, Y. H. Stability augmentation of pitch angle control for maximum power extraction of pmsg-based wts with pitch actuator uncertainty via l1 adaptive scheme. *Int. J. Electr. Power Energy Syst.* **153**, 109392. https://doi.org/10.1016/j.ijepes.2023.109392 (2023).
7. Tang, S., Tian, D., Wu, X., Huang, M. & Deng, Y. Wind turbine load reduction based on 2dof robust individual pitch control. *Renew. Energy* **183**, 28–40. https://doi.org/10.1016/j.renene.2021.10.086 (2022).
8. Saenz-Aguirre, A., Zulueta, E., Fernandez-Gamiz, U., Teso-Fz-Betoño, D. & Olarte, J. Kharitonov theorem based robust stability analysis of a wind turbine pitch control system. *Mathematics* **8**, 85 (2020).
9. Hawari, Q., Kim, T., Ward, C. & Fleming, J. Lqg control for hydrodynamic compensation on large floating wind turbines. *Renew. Energy* **205**, 1–9. https://doi.org/10.1016/j.renene.2023.01.067 (2023).
10. Xie, J., Dong, H. & Zhao, X. Data-driven torque and pitch control of wind turbines via reinforcement learning. *Renew. Energy* **215**, 118893. https://doi.org/10.1016/j.renene.2023.06.014 (2023).
11. Benbouhenni, H. et al. Enhancement of the power quality of dfig-based dual-rotor wind turbine systems using fractional order fuzzy controller. *Expert Syst. Appl.* **238**, 121695. https://doi.org/10.1016/j.eswa.2023.121695 (2024).
12. Wang, Y. & Wang, Z. S. Model free adaptive fault-tolerant tracking control for a class of discrete-time systems. *Neurocomputing* **412**, 143–151 (2020).
13. Zhang, J. & Liu, G. Model-free distributed integral sliding mode predictive control for multi-agent systems with communication delay. *Neurocomputing* **569**, 127133. https://doi.org/10.1016/j.neucom.2023.127133 (2024).
14. Liu, W., Yao, W., Chi, R. & Mu, C. Anti-sway control for bulk terminal gantry cranes based on mfac. In *2023 IEEE 12th Data Driven Control and Learning Systems Conference (DDCLS)* 78–82. https://doi.org/10.1109/DDCLS58216.2023.10165880 (2023).
15. Li, J. Y. et al. Reactive power compensation of 10kv a-line by mcr reactive power compensation device under mfac control strategy. In *2023 8th International Conference on Power and Renewable Energy (ICPRE)* 174–183. https://doi.org/10.1109/ICPRE59655.2023.10353571 (2023).
16. Yao, W., Pei, C., Chi, R., Shao, W. & Li, B. Presynchronization control for ship microgrid of merchant marine inverters based on vsg algorithm with mfac. *Trans. Inst. Meas. Control.* https://doi.org/10.1177/01423312231198922 (2024).
17. Li, J., Wang, S. & Li, Y. A model-free adaptive controller with tracking error differential for collective pitching of wind turbines. *Renew. Energy* **161**, 435–447. https://doi.org/10.1016/j.renene.2020.06.140 (2020).

18. Huang, J., Chen, H. & Shen, C. Event-triggered model-free adaptive control for wheeled mobile robot with time delay and external disturbance based on discrete-time extended state observer. *J. Dyn. Syst. Meas. Contr.* **146**, 021005. https://doi.org/10.1115/1.4063996 (2023).
19. Li, H. et al. Fuzzy optimized mfac based on adrc in auv heading control. *Electronics* **8**, 125. https://doi.org/10.3390/electronics8060608 (2019).
20. Li, T., Yu, Y., Zhang, C. & Zhou, M. Improved mode-free adaptive control for piezoelectric micro-positioning platform. In *2023 6th International Conference on Intelligent Robotics and Control Engineering (IRCE)* 103–107. https://doi.org/10.1109/IRCE59430.2023.10255053 (2023).
21. Liu, S., Jia, X., Ji, H. & Fan, L. Parameter optimization design of mfac based on reinforcement learning. In *2023 IEEE 12th Data Driven Control and Learning Systems Conference (DDCLS)* 1036–1043. https://doi.org/10.1109/DDCLS58216.2023.10167283 (2023).
22. Xu, S. et al. Research on diameter control of czochralski silicon single crystal based on pso parameter tuning for rnn-pfdl-mfac. In *International Conference on Electronic Materials and Information Engineering (EMIE 2023), vol. 12919* 243–251 (SPIE, 2023).
23. Pham, H. A. & Söffker, D. Modified model-free adaptive control using compact-form dynamic linearization technique. *IFAC-PapersOnLine* **53**, 3940–3945. https://doi.org/10.1016/j.ifacol.2020.12.2248 (2020).
24. Corradini, M., Ippoliti, G., Orlando, G. & Corona, D. A data-driven model-free adaptive controller with application to wind turbines. *ISA Trans.* **136**, 267–274. https://doi.org/10.1016/j.isatra.2022.11.002 (2023).
25. Hou, Z. & Jin, S. *Model Free Adaptive Control: Theory and Applications* (CRC Press, 2013).
26. Ahmed, M. R., Damatty, A. E., Dai, K. & Lu, W. Dynamic analysis of horizontal axis wind turbines under thunderstorm downbursts. *J. Struct. Eng.* **149**, 04023143. https://doi.org/10.1061/JSENDH.STENG-11923 (2023).
27. Yang, W.-C., Yang, J.-B., Deng, E., Ni, Y.-Q. & Liu, Y.-K. Aerodynamic behavior of flaky spalled blocks in high-speed rail tunnel lining under slipstream. *Tunn. Undergr. Space Technol.* **141**, 105377. https://doi.org/10.1016/j.tust.2023.105377 (2023).
28. Jonkman, J., Butterfield, S., Musial, W. & Scott, G. Definition of a 5-mw reference wind turbine for offshore system development. In *Tech. Rep., National Renewable Energy Lab.(NREL), Golden, CO (United States)* (2009).
29. Poureh, A., Chamani, M. & Bahri, A. Nonlinear analysis of gain scheduled controllers for the nrel 5-mw turbine blade pitch control system. *Int. J. Electr. Power Energy Syst.* **145**, 108578. https://doi.org/10.1016/j.ijepes.2022.108578 (2023).
30. Liu, S., Han, Y., Ma, R., Hou, M. & Kang, C. A novel composite pitch control scheme for floating offshore wind turbines with actuator fault consideration. *J. Mar. Sci. Eng.* **11**, 748. https://doi.org/10.3390/jmse11122272 (2023).
31. Mihalič, F., Truntič, M. & Hren, A. Hardware-in-the-loop simulations: a historical overview of engineering challenges. *Electronics* **11**, 2462 (2022).

Acknowledgements

The researchers would like to acknowledge the National Natural Science Foundation of China, Grant number 72361033 for funding this work.

Author contributions

S.W. and Z.Z.: Conceptualization. H.L, J.J. and J.Z.: methodology, software, validation. D.Y.: formal analysis, investigation. Z.Z, H.L and S.W.: original draft preparation, project administration, supervision, resources, writing-review and editing. All authors have read and agreed to the published version of the manuscript.

Funding

This research was funded by the National Natural Science Foundation of China (Grant number 72361033).

Competing interests

The authors declare no competing interests.

Additional information

Correspondence and requests for materials should be addressed to S.W.

Reprints and permissions information is available at www.nature.com/reprints.

Publisher's note Springer Nature remains neutral with regard to jurisdictional claims in published maps and institutional affiliations.